Cell

Differentiated *Troy*$^+$ Chief Cells Act as Reserve Stem Cells to Generate All Lineages of the Stomach Epithelium

Daniel E. Stange,[1,2,8] Bon-Kyoung Koo,[1,3,8] Meritxell Huch,[1] Greg Sibbel,[4] Onur Basak,[1] Anna Lyubimova,[1,5] Pekka Kujala,[6] Sina Bartfeld,[1] Jan Koster,[7] Jessica H. Geahlen,[4] Peter J. Peters,[6] Johan H. van Es,[1] Marc van de Wetering,[1] Jason C. Mills,[4] and Hans Clevers[1,*]

[1]Hubrecht Institute for Developmental Biology and Stem Cell Research & University Medical Centre Utrecht, 3584 CT Utrecht, the Netherlands

[2]Department of General, Thoracic and Vascular Surgery, University Hospital Carl Gustav Carus, University of Dresden, 01307 Dresden, Germany

[3]Wellcome Trust - Medical Research Council Stem Cell Institute, University of Cambridge, Cambridge CB2 1QR, UK

[4]Division of Gastroenterology, Department of Medicine, Washington University School of Medicine, St. Louis, MO 63110, USA

[5]Department of Physics & Biology, Massachusetts Institute of Technology, Cambridge, MA 02139, USA

[6]Division of Cell Biology II, Antoni van Leeuwenhoek Hospital/Netherlands Cancer Institute, 1066 CX Amsterdam, the Netherlands

[7]Department of Oncogenomics, Academic Medical Center, University of Amsterdam, 1100 DE Amsterdam, the Netherlands

[8]These authors contributed equally to this work

*Correspondence: h.clevers@hubrecht.eu

http://dx.doi.org/10.1016/j.cell.2013.09.008

SUMMARY

Proliferation of the self-renewing epithelium of the gastric corpus occurs almost exclusively in the isthmus of the glands, from where cells migrate bidirectionally toward pit and base. The isthmus is therefore generally viewed as the stem cell zone. We find that the stem cell marker *Troy* is expressed at the gland base by a small subpopulation of fully differentiated chief cells. By lineage tracing with a *Troy-eGFP-ires-CreERT2* allele, single marked chief cells are shown to generate entirely labeled gastric units over periods of months. This phenomenon accelerates upon tissue damage. *Troy*$^+$ chief cells can be cultured to generate long-lived gastric organoids. *Troy* marks a specific subset of chief cells that display plasticity in that they are capable of replenishing entire gastric units, essentially serving as quiescent "reserve" stem cells. These observations challenge the notion that stem cell hierarchies represent a "one-way street."

INTRODUCTION

The gastric epithelium is a physiologically self-renewing tissue (Mills and Shivdasani, 2011). Anatomically, the stomach can be divided into three parts: the forestomach (in mice) or the cardiac region (in humans), the corpus, and the pyloric region. Invaginations from the inner surface called gastric units or glands penetrate deep into the mucosa and contain distinct cell lineages. In the corpus, the main body of the stomach, gastric units are subdivided further into four distinct zones based on the presence of characteristic cell types. Short-lived (2–3 days) surface mucous cells are the main cell type of the uppermost segment, the pit. Directly below the pit, the isthmus contains immature, fast-dividing cells. Below this, the neck region contains mucous neck cells that are thought to transdifferentiate into chief cells in a period of weeks (Goldenring et al., 2011; Mills and Shivdasani, 2011). Chief cells populate the base and produce digestive enzymes. Scattered throughout all regions are acid-producing parietal cells and rare, hormone-secreting enteroendocrine cells. Chief and parietal cells are long-lived, with an estimated turnover rate of months (Karam and Leblond, 1993a).

Lineage-tracing studies with chemical mutagenesis (Bjerknes and Cheng, 2002) or genetic tracing from the *Sox2* locus (Arnold et al., 2011) have demonstrated the existence of multipotent stem cells in the epithelium. As *Sox2*-positive (*Sox2*$^+$) cells are scattered throughout the isthmus as well as in lower parts of the gastric unit, it is not clear whether all or only a subset of the *Sox2*$^+$ cells can induce stem cell-like lineage-tracing events. Additional markers have been proposed (but not proven by definitive experiments such as, e.g., lineage tracing) for gastric stem cells (Mills and Shivdasani, 2011; Qiao and Gumucio, 2011).

We have recently shown that *Lgr5* marks adult stem cells in the pyloric region of the stomach (Barker et al., 2010). *Lgr5*$^+$ stem cells express a Wnt target gene program, are located at the bottom of pyloric glands, and are capable of long-term renewal of the epithelium. A second pyloric stem cell has been revealed by lineage tracing with a Villin promoter-driven Cre transgene, which identifies a quiescent stem cell of unknown identity that only becomes apparent upon Interferon-γ stimulation (Qiao et al., 2007). Neither of these two studies identified stem cells in the much larger gastric corpus. Based on the predominant location of proliferative cells in the isthmus of the corpus units, it is generally believed that the isthmus represents the stem cell zone of the corpus epithelium (Karam and Leblond, 1993a).

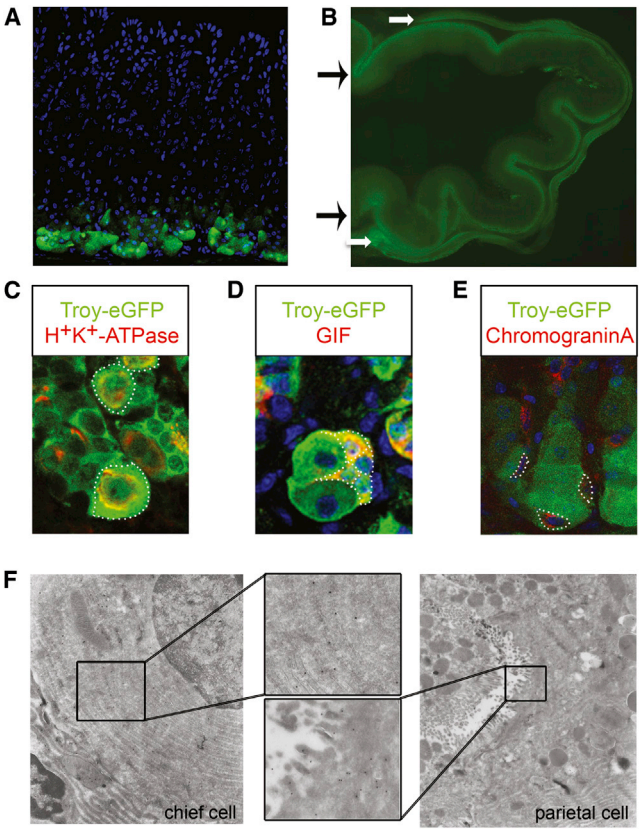

Figure 1. *Troy* Is Expressed in Chief and Parietal Cells at the Base of Corpus Glands

(A) Confocal image showing *Troy-eGFP* expression at the bases of corpus glands in a *Troy-ki* mouse. Projection of six 1 μm spaced z stacks.

(B) *Troy-eGFP* is expressed at gland bottoms throughout the corpus. Black arrows point to the base of the epithelial lining, white arrows to the muscle layer.

(C–E) Confocal microscopy reveals that *Troy-eGFP*$^+$ cells are coexpressing either the parietal cell marker H^+K^+-ATPase (C) or the chief cell marker GIF (D). Basal enteroendocrine cells marked by chromogranin A are *Troy-eGFP*$^-$ (E).

(F) Electron microscopy of cryo-immunogold-labeled *Troy-eGFP*$^+$ cells. Fifteen nanometer gold label corresponding to *eGFP* are visible as black dots. Both chief and parietal cells at the gland base express *eGFP*, and positive cells possess characteristics of maturation specific to that lineage.

See also Figure S1.

RESULTS

Identification of *Troy* as a Stem Cell Marker in Multiple Adult Tissues

Following the identification of Lgr5 as a marker of adult stem cell populations in small intestine and colon, we have established transcriptional profiles of Lgr5$^+$ stem cells (Muñoz et al., 2012; van der Flier et al., 2009). One of the genes that closely followed the expression pattern of *Lgr5* in intestinal crypts was *Troy* (encoded by *Tnfrsf19*). *Troy* potentially functions as a receptor for lymphotoxin A (Hashimoto et al., 2008). It is highly homologous to two other Tnfrsf members, *Xedar* and *Edar*. *Troy* knockout mice are viable and fertile without an obvious phenotype (Shao et al., 2005). A recent study has confirmed that *Troy* marks intestinal stem cells (Fafilek et al., 2013). Interestingly, *Troy* expression does not correlate with *Lgr5* expression in nonintestinal Lgr5$^+$ stem cell populations (Barker et al., 2010; Jaks et al., 2008). As *Troy* may mark novel *Lgr5*-independent sets of adult stem cells, we generated a *Troy-eGFP-ires-CreERT2* knockin mouse line (*Troy-ki*), in which *eGFP* and *CreERT2* are under the control of endogenous *Troy*-regulatory sequences (Figure S1A available online).

Expression of *eGFP* occurred in crypt base columnar cells, the *Lgr5*$^+$ stem cells of the small intestine (Figure S1B). In vivo lineage tracing performed in *Troy-ki* mice crossed with the *R26R-LacZ* Cre reporter strain resulted in typical "ribbons," confirming recently published data (Fafilek et al., 2013) (Figure S1C). As expected, lineage tracing was not observed in *Lgr5*$^+$ stem cell compartments that were *Troy* negative (*Troy*$^-$), i.e., in the colon or gastric pylorus. However, tracing events occurred in the gastric corpus, kidney, liver, lung, and brain. For here, we focused on the gastric corpus.

Troy Is Expressed Specifically at the Base of Gastric Corpus Units

Troy-eGFP expression was readily detectable at the base of each gastric corpus unit (Figures 1A and 1B), faithfully recapitulating the endogenous expression of *Troy*. Single-molecule in situ hybridization (Itzkovitz et al., 2012) detected *Troy* messenger RNA (mRNA) in chief and parietal cells at gland bases, whereas cells of the same types, yet located higher up toward the neck region, were *Troy*$^-$ (Figure S1D). Of note, the muscle layer of the stomach also expressed *Troy* (Figure 1B, white arrow). Double-immunofluorescent stainings confirmed the expression of *Troy-eGFP* in chief and parietal cells at the gland base. *Troy-eGFP*$^+$ cells colabeled either with H^+K^+-ATPase, a marker for parietal cells, or with gastric intrinsic factor (Gif), a marker for chief cells in mice (Figures 1C and 1D), whereas the third cell type present at the bottoms of corpus glands, the enteroendocrine cell, was *Troy*$^-$ (Figure 1E).

Next, electron microscopy was employed to resolve the ultrastructure of *Troy*$^+$ cells. Cryo-immunogold labeling detected the *eGFP* marker in both chief and parietal cells at the gland base (Figure 1F). Quantification showed an average of 3.9 and 3.5 eGFP-gold particles/1 μm^2 in chief cells and parietal cells, respectively. No eGFP-gold label was detected in the same cell types higher up in the gastric unit or in enteroendocrine cells at the gland bottom (Figures S1E and S1F). The marked cells showed characteristics of mature chief and parietal cells, i.e., extending basal rER cisternae and light homogeneous secretory granules in chief cells and a central nucleus surrounded by the intracellular canaliculus and mitochondria-filled cytoplasm in parietal cells (Karam, 1993; Karam and Leblond, 1993b).

Lineage Tracing Reveals that *Troy*$^+$ Cells Act as Multipotent Stem Cells of the Gastric Corpus

Lineage tracing initiated in 8-week-old mice induced single LacZ$^+$ cells at the bottoms of corpus glands 1 day post-induction (p.i.) (Figure 2A). A slow clonal expansion over time was apparent. Indeed, historic labeling experiments with tritiated thymidine (^{3}H-TdR) have indicated that proliferating cells with chief cell characteristics exist at the gland bottom (Chen and

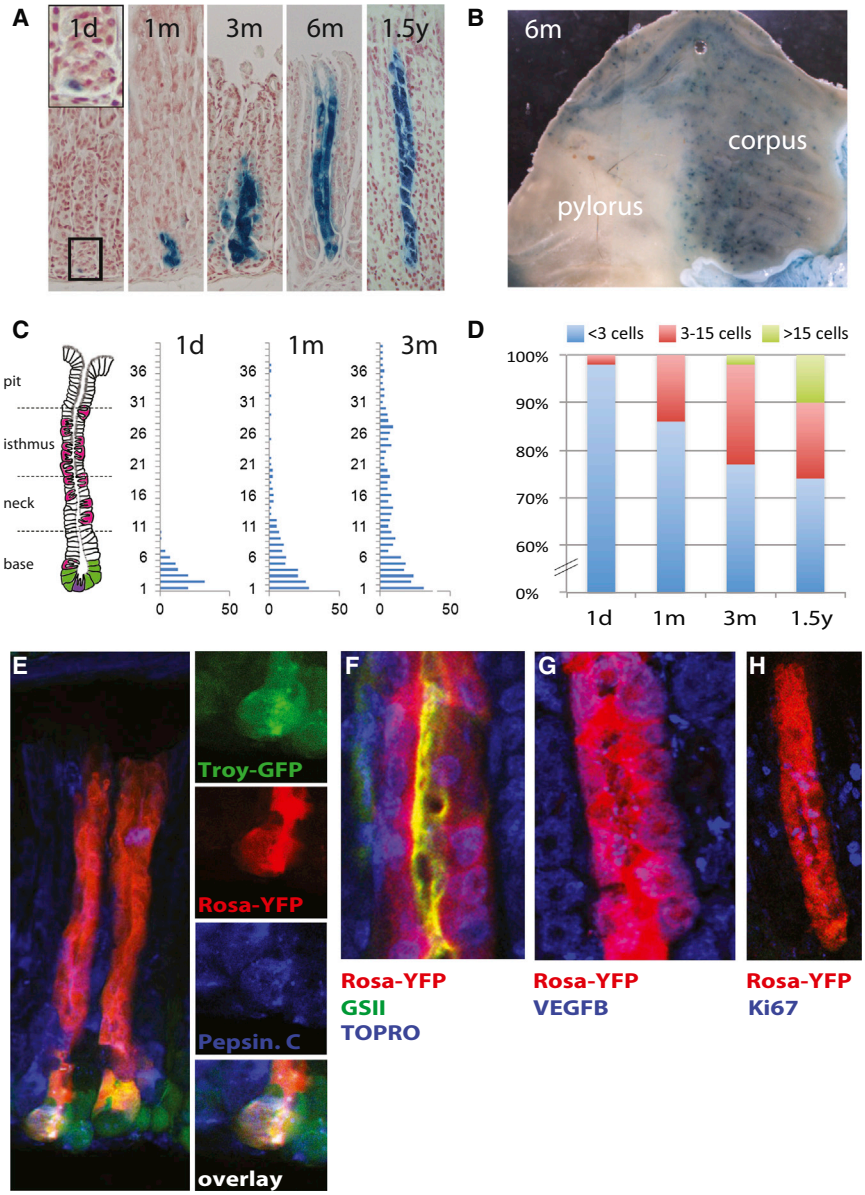

Figure 2. *Troy*$^+$ Cells Generate All Lineages

(A) Expression of the *Rosa-LacZ* reporter gene in *Troy*$^+$ cells one day p.i. and followed for 1, 3, and 6 months and 1.5 years p.i.

(B) Whole-mount LacZ staining of *Troy-ki* stomach 6 months p.i. Lineage tracing is evident in the corpus; pylorus is negative.

(C) The position of LacZ$^+$ cells quantified for 100 tracing clones at 1 day, 1 month, and 3 months p.i..

(D) Numbers of LacZ$^+$ cells in 100 tracing clones counted at 1 day, 1 month, 3 months, and 1.5 years p.i. as percentage of clones with < 3, 3–15, and > 15 cells.

(E–H) Double/triple immunofluorescence stainings for corpus lineage markers on *Troy-ki;Rosa-YFP* mice: chief cells (pepsinogen C, E), mucus neck cells (GSII, F), parietal cells (VEGFB, G), and isthmus cells (Ki67, H).

See also Figures S2 and S3.

Withers, 1975; Willems et al., 1972). We performed triple-immunofluorescent stainings for *Ki67* and *pepsinogen C* together with a membrane marker, and confirmed the existence of rare, dividing chief cells at the bottoms of glands (Figure S2A). On average, 3.2% ± 0.78% of corpus glands contained a proliferative cell at the gland base (Figure S2B). Thus, despite the fact that the isthmus appears to be the principle zone of proliferation, a second zone with the capability to proliferate exists at the bottom of glands.

Eventually, lineage tracing yielded clones of LacZ$^+$ cells spanning the entire length of a gland. This was rarely observed at 4 weeks of tracing yet became more frequent from 3 month onward (Figures 2A and 2B). Of note, no tracing was detected in the pyloric region, consistent with the absence of *Troy-eGFP*$^+$ cells (Figure 2B). Entirely traced gastric units persisted at least up to 1.5 years, the latest time point examined (Figure 2A). Besides the expanding clones, a fraction of cells remained as single LacZ$^+$ cells at the bottoms of glands (Figure S3A, arrows). Staining for the parietal cell marker H$^+$K$^+$-ATPase on tissue sections from 6 month tracing experiments revealed that these nonexpanding single LacZ$^+$ cells were parietal cells (Figure S3B), whereas all early expanding clones contained chief cells (Figure S3C). Control noninduced *Troy-ki/R26R-LacZ* did not show LacZ$^+$ cells at any time point (Figure S3D). Furthermore, induction of lineage tracing according to our standard protocol did not result in parietal cell loss, unlike what has been reported in other models (Huh et al., 2012) (Figure S3E).

Quantification of clone size in tracing clones containing only parietal cells and clones containing chief cells (only chief cells or mixed chief/parietal clones) was performed. Pure parietal cell clones did not grow; the average clone size after 1 week and 3 months was 1.1 and 1.3 ± 0.1 cells, respectively. On the other hand, clones containing chief cells increased in size from an average of 1.9 ± 0.1 to 3.6 ± 0.8 cells/clone at 3 months. This suggested that growth of clones originated from the chief cell population. The position of LacZ$^+$ cells was quantified for 100 glands over a 3 month time course (Figure 2C). At day 1 p.i., we never detected a LacZ$^+$ cell above position 10 from the bottom (this position is still > 10 cell positions below the lower isthmus region). Progressively, the number of LacZ$^+$ cells higher up in the gland increased. The clone size was quantified in 100 glands over a 1.5 year time course p.i. An increase in clone size could be observed (Figure 2D). The rate of expansion was relatively slow, with an average doubling time of clone size of around 50 days. This fitted well with the

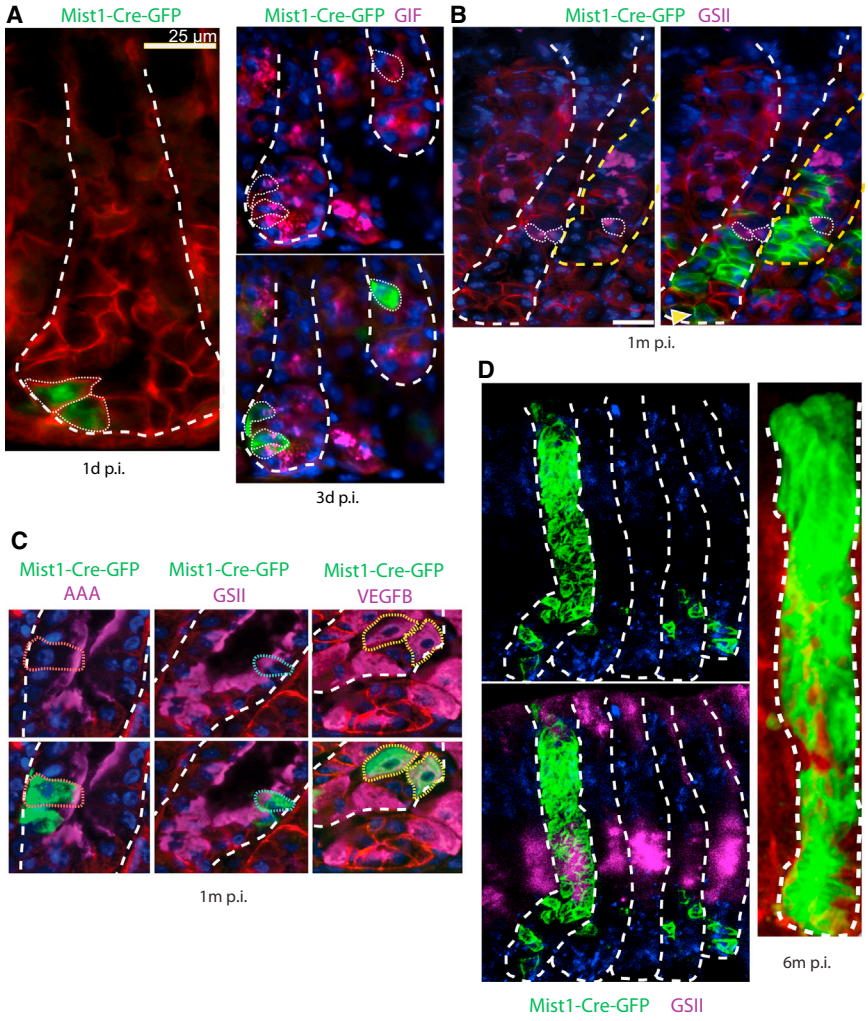

Figure 3. *Mist1*$^+$ Cells Generate All Lineages

(A) One and three days following *Mist1-CreERT2* induction (p.i.), typical corpus gastric units show 1–3 *Rosa-mTmG* reporter-positive epithelial cells, which label with the chief cell marker GIF.

(B) One month p.i., the vast majority of *Mist1* lineage-traced cells (green) are basal, *GSII* (purple) negative chief cells.

(C) Occasionally, at 1 month p.i., *Mist1*$^+$ cells generate AAA$^+$ pit cells, *GSII*$^+$ mucus neck cells, and VEGFB$^+$ parietal cells.

(D) At 6 months p.i., entirely marked corpus units can be detected, encompassing the *GSII*-marked mucous neck cells (staining of lumenal cells is background), the isthmus, and the pit region. Zeiss ApoTome (left) and multiphoton (right) technology were used to visualize units as z stack reconstructions from thick tissue sections.

observation that chief cells double in 2 months, as analyzed by grain count analysis after ^{3}H-TdR administration (Willems et al., 1972).

Within LacZ$^+$ ribbons that had grown beyond the isthmus, all differentiated cell types of the gastric corpus were detected, i.e., chief cells, neck cells, parietal cells, proliferating isthmus cells, pit cells, and enteroendocrine cells (Figures 2E–2H and S3F). We concluded that a *Troy*$^+$ cell with the capacity to generate all stomach epithelial cell types exists at the bottom of glands in the adult gastric corpus.

We repeated the tracing experiments using the Cre knockin line *Mist1-CreERT2*, which is expressed only in mature chief cells (Nam et al., 2010; Shi et al., 2009). These mice were crossed with the Rosa-mTmG reporter line (Figure 3). Induction of Cre activity led to the GFP labeling of 1–3 chief cells in the gland base (Figure 3A). One month later, rare tracing events were observed (Figure 3B). Traced clones consisted mainly of chief cells and were located at gland bottoms, typically containing at least one cell located at the very base, overlapping with the *Troy* expression domain (Figure 3B, arrow). Already within these early tracing units, all principal differentiated cell types of the gastric epithelium were detected (Figure 3C). Lineage tracing proceeded as observed for the *Troy* locus. At 6 months, tracing units spanning entire corpus glands were readily detectable (Figure 3D).

Troy$^+$ Chief Cells Express Markers of Chief Cells and Wnt-Driven Stem Cells

We isolated *Troy*$^+$ chief cells by fluorescence-activated cell sorting (FACS) (described below; see Figure 6A) to analyze their transcriptional program. *Troy*$^+$ chief cells comprised around 0.9%, whereas *Troy*$^+$ parietal cells accounted for 0.5% of all epithelial corpus gland cells. Three independent sorts were performed, and mRNA analyzed on microarrays. On average, *Troy* mRNA was found to be 7.3-fold enriched in sorted GFP$^+$ chief cells compared to whole corpus glands, further validating the recombinant *Troy* allele.

We first compared our arrays by unsupervised hierarchical clustering to arrays representing the three main lineages of the stomach (pit, parietal, and chief cells) (Ramsey et al., 2007). The *Troy*$^+$ arrays clustered together with the chief cell array, whereas the pit and parietal cell arrays separated in a different tree (Figure 4A). The overall chief cell signature was therefore maintained in the *Troy*$^+$ subpopulation. *Troy*$^+$ chief cells showed enrichment for the chief cell markers *Gif* and *Mist1* (Figure 4B). We also detected enrichment in genes previously detected in small intestinal or pyloric stem cells, i.e., *Lgr5*, *Ascl2*, *Lrig1*, and *Rnf43*/*Znrf3* (Barker et al., 2007; Koo et al., 2012; van der Flier et al., 2009; Wong et al., 2012). In addition to the Wnt target genes *Lgr5, Ascl2*, and *Rnf43*/*Znrf3,* several other well-characterized Wnt target genes were expressed, i.e., *Axin2*, *EphB2*, and *Cd44* (Van der Flier et al., 2007) (Figure 4B). Overall, 113 genes were found to be significant and more than 2-fold enriched in *Troy*$^+$ chief cells compared to whole corpus glands (Table S1).

The detection of active Wnt signaling in the adult gastric corpus was surprising, as this pathway has until now only been associated with the pyloric region (Mills and Shivdasani, 2011). The enrichment of the Wnt signature and intestinal stem cell marker genes in *Troy*$^+$ chief cells was first confirmed by quantitative PCR (qPCR) (Figure 4C). Next, we compared the levels of Wnt activity between corpus glands, pylorus, and small intestine by performing qPCR of *Axin2* (Figure 4D). The overall level of Wnt activity was highest in the small intestine, 10-fold lower in the pylorus, and lowest in corpus glands. The intestinal and pyloric stem cell marker *Lgr5* was detected at similar levels in small intestine and corpus, while being highest in the pyloric region. *Axin2-LacZ* mice (Lustig et al., 2002) showed strong LacZ positivity at the bases of pyloric glands. In addition, these mice revealed Axin2$^+$ cells in the corpus (Figure 4E). As the *Lgr5-eGFP-ires-CreERT2* mouse (Barker et al., 2007) did not show Lgr5 expression in the corpus region, contrary to our array and qPCR data, we examined expression in an independent Lgr5 reporter, the *Lgr5-DTR:eGFP* mouse (Tian et al., 2011). In this line, Lgr5 expression was readily detectable at the bases of corpus glands (Figure 4F).

We used gene set enrichment analysis (GSEA) to statistically test whether *Troy*$^+$ chief cells express only a few marker genes (Figures 4B and 4C) or—more broadly—the signature of intestinal/pyloric stem cells, of chief cells, and of the Wnt pathway. GSEA revealed significant enrichment of all four gene sets in *Troy*$^+$ chief cells (Figures S4A–S4D). Gene sets for parietal and pit cells were negatively correlated with those for *Troy*$^+$ chief cells (Figures S4E and S4F). In summary, the transcriptional program of *Troy*$^+$ chief cells combines chief cell-specific genes with genes previously described as Wnt-dependent stem cell genes.

Single *Troy*$^+$ Chief Cells Can Form Long-Lived Organoids that Differentiate toward Mucus Neck and Pit Cells

We have previously established a long-term culture system that allows unlimited expansion from single *Lgr5*$^+$ pyloric stem cells (Barker et al., 2010). To test whether similar epithelial organoid cultures can be established from the corpus epithelium, we attempted to culture freshly isolated, entire corpus units. Within a few hours after seeding, the units disaggregated. Subsequently, rare cells typically located at the bottom of the gland units started to proliferate and form cystic structures (Figure 5A). To investigate whether the cultures were derived from *Troy*$^+$ cells, we induced tracing in vivo in *Troy-ki* crossed with *Rosa-YFP* Cre reporter mice 3 days before the isolation of glands. We then followed the expression of YFP in the developing organoids in vitro. Initially, YFP and GFP signals overlapped (Figure 5B). In the course of a week, the YFP-tracing clones continuously expanded, contributing significantly to the cell mass of growing organoids (Figure 5C).

We next tested whether single *Troy*$^+$ cells isolated from gastric units of the corpus were also capable of generating organoids. Two populations of *Troy*$^+$ cells, different in scatter properties, were observed with FACS (Figure 6A). Stainings for lineage markers on sorted cells showed that the "small cell" population (gate A) consisted of chief cells, whereas the population containing larger cells (gate B) represented parietal cells (Figure 6B). *Troy*$^+$ chief cells consistently grew out into organoids (colony-forming efficiency 5.4%) (Figure 6C). We followed a single sorted chief cell over a period of 6 month, by weekly passaging at a 1:6 ratio (Figure 6D). No change in growth behavior was apparent over the culture period. Similarly, single sorted *Mist1*$^+$ chief cells could initiate organoid growth (Figures S5A and S5B). In contrast, *Troy*$^+$ parietal cells died within 1–2 days of culture (Figure 6C). Immunohistochemistry (IHC) demonstrated a high proliferative activity of *Troy*$^+$-derived organoids (Figure 6E). Double stainings revealed the presence of proliferative chief cells (Figure 6F). Besides chief cells, we noted a distinct population of cells expressing the epitope for GSII, a marker for mucus neck cells (Figure 6G). A similar expression pattern of mucous neck, chief, and proliferation markers has been described in a two-dimensional (2D) chief cell culture (Tashima et al., 2009).

A small proportion of *Troy*$^-$ cells (0.4%) was also able to generate corpus organoids (Figure 6C). To exclude contamination of *Troy*$^-$ by *Troy*$^+$ cells, we examined *Troy*$^-$-derived organoids from *Troy-ki/Rosa-YFP* mice (Figure 6H). FACS-isolated single *Troy*$^-$ and *Troy*$^+$ cells were induced in vitro with tamoxifen right after initiation of culture. No yellow fluorescent protein (YFP) was detected in *Troy*$^-$-derived organoids, whereas YFP was expressed throughout *Troy*$^+$-derived organoids. Phenotypically, *Troy*$^-$-derived organoids showed a more cystic growth behavior with fewer buddings during the first four passages (Figure 6I). *Troy* mRNA expression was hardly detectable in *Troy*$^-$-derived organoids (Figure S5C). During subsequent passages, growth characteristics of *Troy*$^-$- and *Troy*$^+$-derived organoids became indistinguishable. Of note, only 2/3 of initially growing *Troy*$^-$-derived organoids could be propagated for more than three passages, whereas all *Troy*$^+$-derived organoids grew without constraints.

To further test the differentiation capacity of the *Troy*$^+$-derived organoids, we removed several mitogenic growth factors (Fgf10, Noggin, and Wnt3a) from the culture medium (termed ERG medium). Microarraying of organoids derived from a single *Troy*$^+$ chief cell grown in normal (termed ENRGFW) medium revealed the expression of markers of intestinal and pyloric stem cells (i.e., *Lgr5*, *Ascl2*, *Rnf43*, and *Troy*), chief cells (i.e., *Mist1, Gif*, and *Pgc*) as well as proliferative cells (i.e., *Ccnb2* and *Ki67)* (Figures S5D and S5F) (Barker et al., 2007; Koo et al., 2012; van der Flier et al., 2009). Upon withdrawal of the mitogenic factors, a profound upregulation of markers for pit cells (i.e., *Muc5ac* and *Gkn1)* was detected (Figures S5E an S5G), indicating that *Troy*$^+$ chief cells have the capability to generate pit cells, the second mucus-secreting cell lineage in the gastric corpus. We did not detect expression of markers for parietal or enteroendocrine lineages.

Troy$^+$ Stem Cells Are Activated by Depletion of the Proliferating Isthmus Compartment

Compared to the rate of tracing from *Lgr5*$^+$ cells in the pylorus, tracing from the *Troy*$^+$ cells followed much slower kinetics. Although occasional tracings spanning entire gastric units could be found within 1 month p.i., most tracings progressed slowly (Figures 2A and S3C). Proliferating chief cells were rare in the bottom part of glands (Figures S2A and S2B), whereas the isthmus region was constantly cycling (Figure 7A). *Troy*$^+$ stem cells therefore appeared largely dispensable for physiological

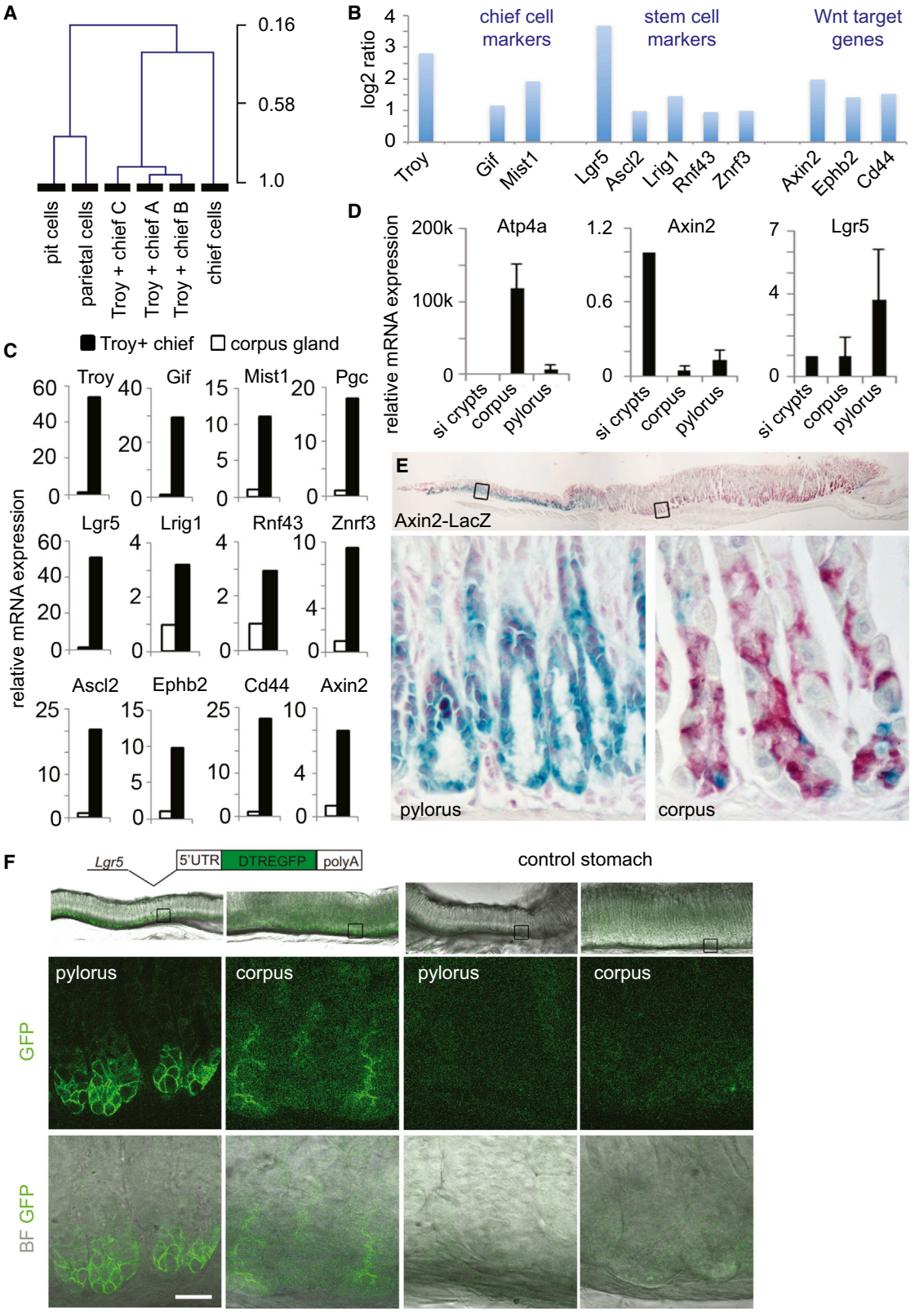

(legend on next page)

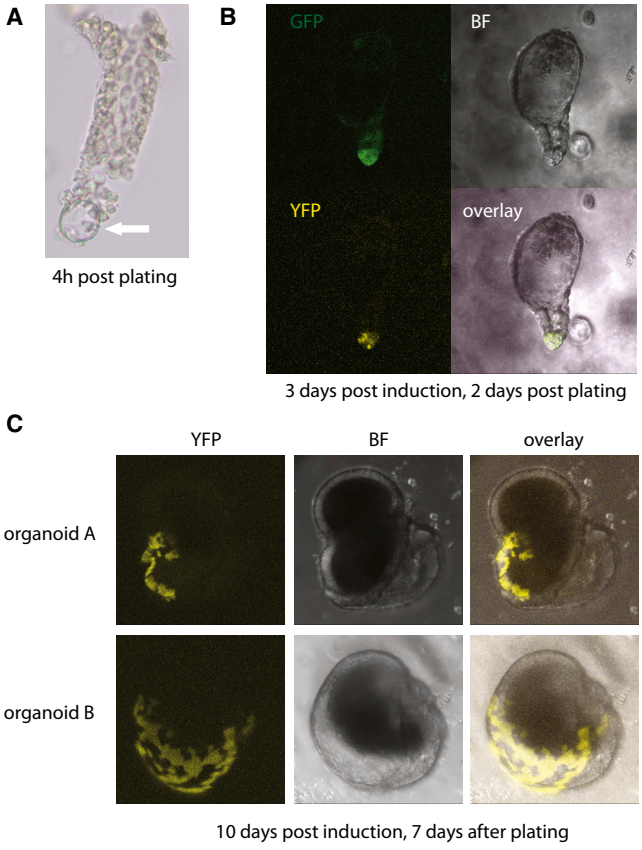

Figure 5. Lineage Tracing from In Vivo to In Vitro Reveals *Troy*$^+$ Cells as the Origin of Corpus Organoids

(A) Freshly isolated corpus unit 4 hr after seeding. The unit already starts to degenerate. Note the small cystic structure at the bottom of the gland (arrow).

(B) Tracing was induced in *Troy-ki/Rosa-YFP* reporter mice 3 days before isolation of corpus glands. Two days after seeding, GFP and YFP signal still overlap, indicating that the tracing clone was still restricted to the *Troy*$^+$ population.

(C) One week after seeding, the YFP clones had expanded and occupied large parts of the organoid.

renewal of the corpus epithelium, rather acting like a "reserve" stem cell population.

To test this hypothesis, we used 5-fluoruracil (5-FU) to selectively kill the proliferative cells in the gastric corpus. This approach has been successfully employed in the bone marrow (Lerner and Harrison, 1990). We induced tracing by tamoxifen administration followed by injection of a single dose of 5-FU 3 days later in the treatment (but not the control) group (Figure 7K). A single dose of 150 mg/kg was enough to completely abolish proliferation in the corpus epithelium (Figure 7D) 2 days post 5-FU injection, whereas *Troy*$^+$ cells, consistent with their slowly cycling nature, appeared unaffected (Figures 7B and 7E). We did not detect any significant change in the composition of the other lineages (Figure S3E). Apoptosis was mainly observed in the isthmus region (Figures 7C and 7F).

The first sign of a contribution of *Troy*$^+$ chief cells to regeneration after 5-FU was seen after 7 days. The percentage of glands with proliferating, *Ki67*$^+$ cells at the gland bottom increased 3-fold from 3.2% ± 0.8% to 10.5% ± 0.9% (Figure S2B). Cell-cycle dynamics at the gland bottom were further analyzed with a double thymidine-analog label-retention experiment. Administration of BrdU (2 weeks of labeling followed by a 3 week chase) and EdU (three times within 6 hr before sacrifice) resulted in BrdU-retaining cells at the gland bottoms (Figure S2C). These cells could be induced to proliferate again upon 5-FU damage, resulting in BrdU;Edu double-positive cells (Figure S2C, right panel). Dividing gland bottom cells therefore can re-enter the cell cycle.

Four weeks after 5-FU treatment, accelerated expansion of LacZ$^+$ clones was evident (Figures 7G–7J). The number of tracing events that reached the gastric lumen increased 6-fold after 5-FU treatment, as compared to the untreated controls (Figure 7H, iii and 7I). Quantification of the size of tracing units clearly showed a shift toward larger units in 5-FU-treated mice (Figure 7J).

DISCUSSION

In this study, we assess *Troy* as a marker of cells that contribute to tissue renewal in the gastric corpus. We find that *Troy* is expressed by a small subset of chief cells and parietal cells located at the gland base. Under steady-state conditions, these cells phenotypically fulfill all requirements of differentiated cells. It was recognized 40 years ago that rare cells with chief cell characteristics and located at the bottom of corpus glands can incorporate radiolabeled thymidine (Chen and Withers, 1975; Willems et al., 1972). Indeed, when *Troy*$^+$ chief cells are cultured in vitro, they vigorously proliferate, while initially maintaining a chief cell-specific gene expression profile. Thus, albeit fully mature, *Troy*$^+$ chief cells have the capacity to undergo cell division. This phenomenon is not without precedent. Mature hepatocytes, for instance, are also capable of re-entering the cell cycle upon

Figure 4. Transcriptional Profile of *Troy*$^+$ Chief Cells

(A) Unsupervised hierarchical clustering joins the *Troy*$^+$ chief cell arrays with a chief cell array prepared from laser-captured chief cells, while pit and parietal cell arrays cluster in a separate tree (data taken from Gene Expression Omnibus data set GSE5018; Ramsey et al., 2007).

(B) Log_2 ratio of selected genes comparing the *Troy*$^+$ chief cell arrays to arrays from whole corpus glands. *Troy*$^+$ chief cells show enrichment of marker genes for chief cells, digestive tract stem cells, and Wnt target genes.

(C) qPCRs performed on a separately sorted set of *Troy*$^+$ chief cells and compared to corpus glands (set to 1) confirm enrichment of all marker genes depicted in (B) in *Troy*$^+$ chief cells. Data are represented as mean ± standard error of the mean (SEM) of three qPCRs.

(D) Comparison of the expression level of the Wnt target gene *Axin2* and the stem cell marker *Lgr5* between small intestine, gastric corpus, and pylorus. Data are represented as mean ± SEM of three qPCRs.

(E) LacZ staining of the *Axin2-LacZ* reporter mouse documents expression of *Axin2* in a few gland bottom cells in the gastric corpus (nuclear red counter stain).

(F) Endogenous eGFP expression in the *Lgr5-DTR:eGFP* reporter mouse visualizes *Lgr5* expression at the bottoms of gastric corpus glands.

See also Figure S4 and Table S1.

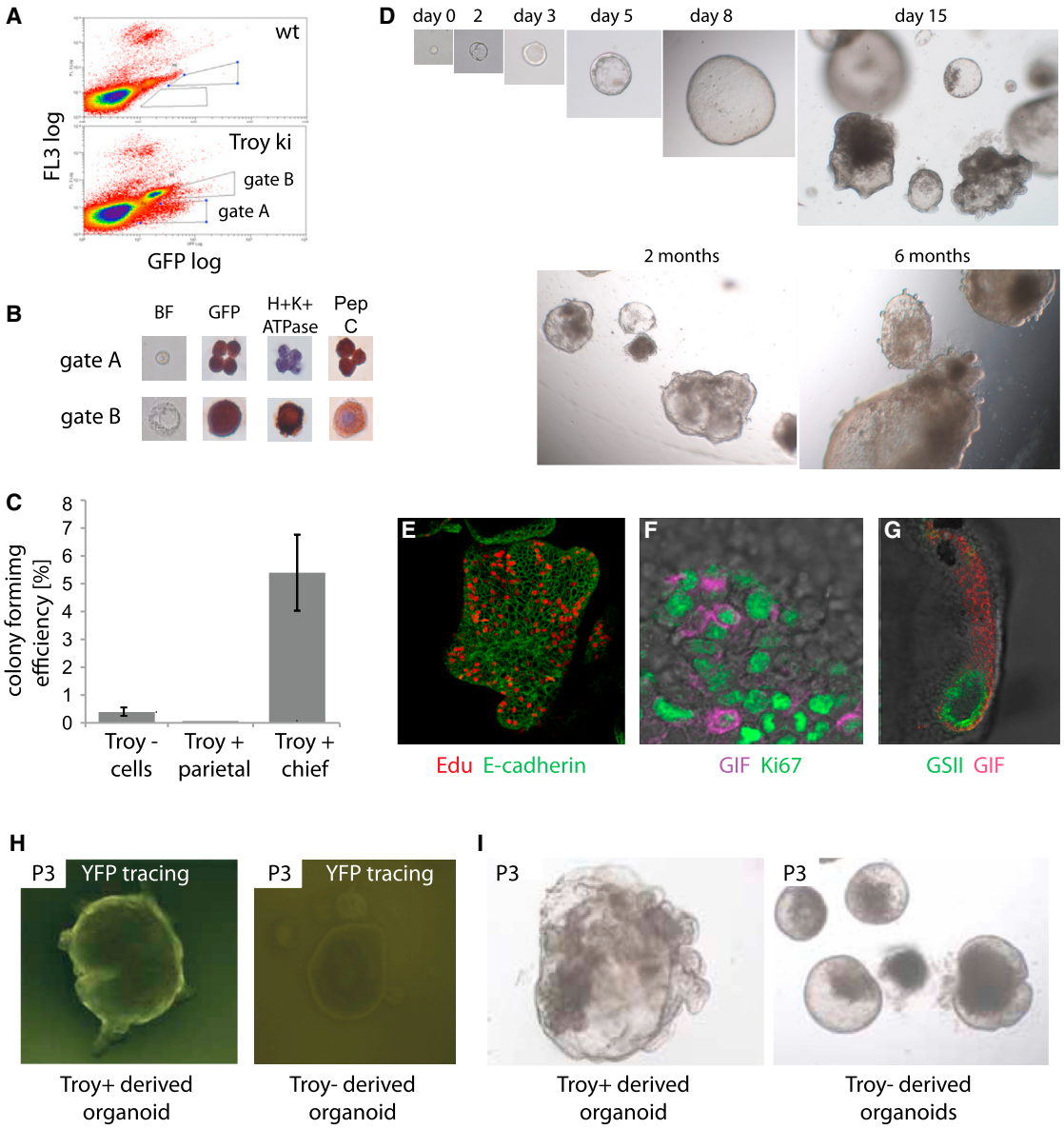

Figure 6. Single *Troy*$^+$ Cells Generate Gastric Organoids In Vitro

(A) Two different populations of *Troy-eGFP*$^+$ cells can be distinguished by FACS (gate A and gate B).

(B) Sorted "gate A" *Troy-eGFP*$^+$ cells stain with chief cell marker pepsinogen C. Gate B *Troy-eGFP*$^+$ cells express parietal cell marker H^+K^+-ATPase.

(C) Colony formation efficiency of *Troy*$^+$ chief and parietal cells as well as *Troy*$^-$ cells. The number of organoids was counted at day 7 after seeding. Data are represented as mean ± SEM of 180 seeded wells.

(D) Representative example of a single sorted and cultured *Troy*$^+$ chief cell. Organoids were passaged weekly and grown for > 6 months.

(E) Organoids are highly proliferative. Edu: proliferative cells; cell borders marked by E-cadherin.

(F) Dividing (*Ki67*$^+$) chief cells (*GIF*$^+$) occur frequently.

(G) Mucus neck cells (*GSII*$^+$) cells form a coherent distinct domain.

(H) Organoids from single sorted *Troy-GFP*$^+$ and *Troy-GFP*$^-$ cells from *Troy-ki/Rosa-YFP* mice were induced by Tamoxifen during the first 16 hr of culture. *Troy-GFP*$^+$-derived organoids were homogenously YFP$^+$, whereas *Troy-GFP*$^-$-derived organoids were YFP$^-$.

(I) *Troy-GFP*$^+$ consistently showed a more complex growing behavior then *Troy-GFP*$^-$-derived organoids.

See also Figures S5 and S6.

partial hepatectomy and resume cell division (Fausto, 2000; Michalopoulos and DeFrances, 1997). Adult Schwann cells have recently been shown to possess a degree of plasticity. When infected with leprosy bacilli, differentiated Schwann cells are induced to convert toward a mesenchymal progenitor/stem-like phenotype (Masaki et al., 2013).

Troy$^+$ chief cells eventually produce all epithelial lineages present in the corpus in vivo and can generate stomach organoid

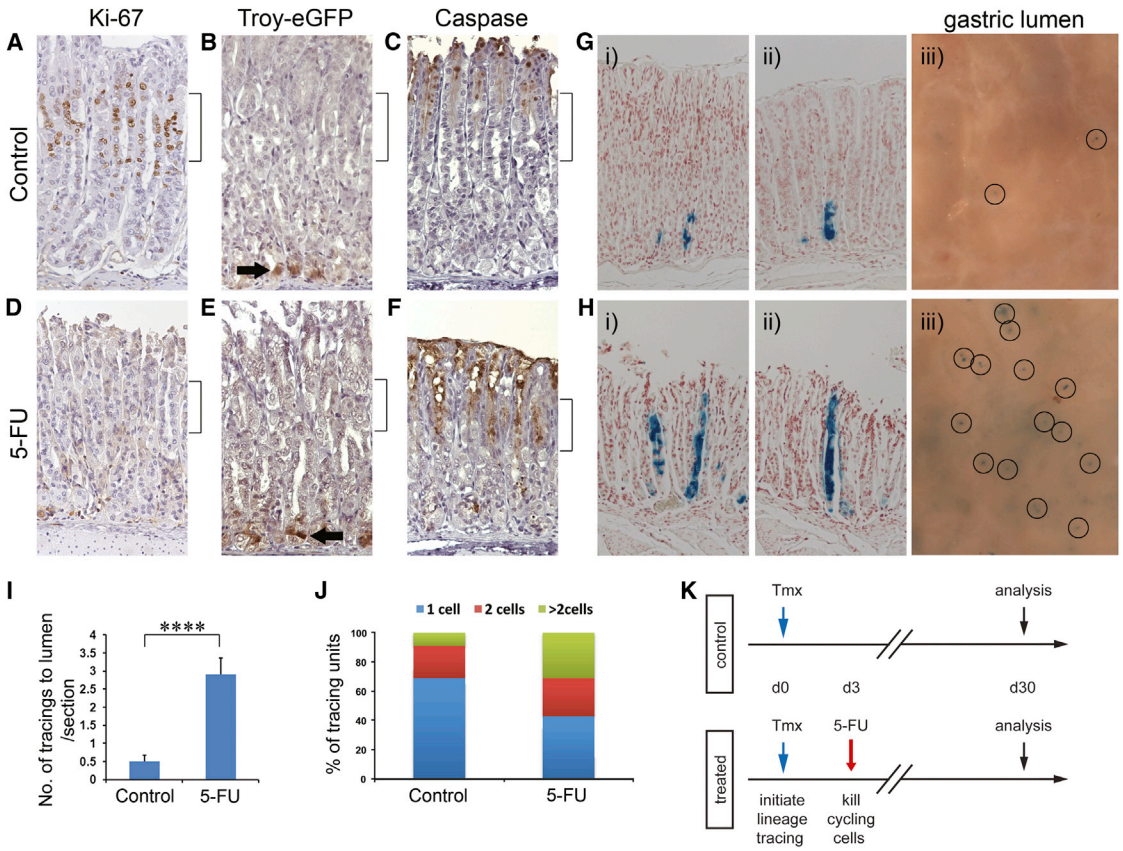

Figure 7. *Troy*$^+$ Chief/Stem Cells Activated by Depletion of Cycling Isthmus Cells

(A–F) 5-FU treatment ablates proliferating cells in the isthmus. Control (A–C) and 5-FU-treated (D–F) mice were analyzed for Ki-67 (A and D, for proliferating cells), GFP (B and E, for *Troy*$^+$ cells), and cleaved caspase 3 (C and F, for apoptotic cells). 5-FU induces apoptosis of cycling isthmus cells.

(G and H) Accelerated expansion of Troy initiated lineage tracing upon tissue damage. Control (G) and 5-FU-treated (H) mice were analyzed 1 month p.i. Representative examples of Troy tracings (i and ii) and whole-mount pictures from the gastric lumen (iii) are shown. Circles indicate LacZ$^+$ glands reaching the lumen.

(I) The number of tracings that reach the lumen was counted 1 month p.i. in 5-FU-treated versus untreated mice and shows a 6-fold increase ($p < 0.0001$, t test). Data are represented as mean ± SEM of ten sections.

(J) The number of LacZ$^+$ cells in 100 tracing clones counted 1 month after 5-FU treatment. Percentages of clones with one, two, or more than two cells are represented.

(K) Time scheme of 5-FU experiment. *Troy*$^+$ cells were labeled on day 0 by tamoxifen induction. Proliferative cells were subsequently ablated by 5-FU treatment 3 days later, and tissues analyzed at 1 month p.i.

cultures that can be differentiated toward the mucus-producing cell lineages of the neck and pit in vitro. Their slowly cycling nature as well as their potential to be activated upon selective killing of the highly proliferative isthmus cells are reminiscent of quiescent/"reserve" tissue stem cells (Li and Clevers, 2010). *Troy*$^+$ chief cells are unique among chief cells in expressing a large number of Wnt target genes. This implies that a source of Wnt is located near the gland bottom, much like in the pylorus, small intestine, and colon. It will be interesting in the future to dissect the factors that build the niche for *Troy*$^+$ chief cells. Besides the underlying mesenchyme, a potential niche cell candidate are the *Troy*$^+$ parietal cells intermingled between the *Troy*$^+$ chief cells at the gland bottom.

How do these *Troy*$^+$ stem cells compare to previously identified gastric stem or progenitor cells in the corpus? In contrast with *Troy*$^+$ cells, *Sox2*$^+$ stem cells are scattered within and below the isthmus and do not express known differentiation markers (Arnold et al., 2011). We observed that almost all epithelial cells within the normal stomach as well as in the organoids express *Sox2* (Figure S6). We also do see clear expression of *Sox2* in *Troy*$^+$ chief cells in our array data with no difference compared to whole corpus glands ($p = 0.41$). Within the isthmus, *Tff2*-expressing cells have been demonstrated to represent progenitors of chief and parietal cells, but not of mucous-secreting pit cells and enteroendocrine cells (Quante et al., 2010). Besides the immediate labeling of parietal cells, *Tff2*-driven lineage tracing results in the labeling of mucous neck cells and—later—in the labeling of chief cells. This delay agrees with the view that chief cells can be generated by transdifferentiation of mucous neck cells (Goldenring et al., 2011). Although this has not been unequivocally proven by lineage tracing of mucous neck cells, substantial indirect evidence exists to support this concept (Goldenring et al., 2011). This evidence is based on findings that, first, nucleotide analogs after administration are initially

seen in mucous neck cells and only afterward in chief cells (Karam and Leblond, 1993b). Second, the deletion of the chief cell transcription factor *Mist1* or its upstream transcriptional regulator *Xbp1* results in the accumulation of cells with mixed chief-neck cell characteristics, whereas neck cells are normal, indicating a block in transdifferentiation (Bredemeyer et al., 2009; Huh et al., 2010; Ramsey et al., 2007). The current finding might constitute a reversion of this process, a retransformation into mucous neck cells and then into isthmus cells.

In accordance with our observation of *Troy*$^+$ chief cell activation upon 5-FU treatment is the fact that chief cells at the bottom of glands can be activated upon the specific loss of parietal cells (Bredemeyer et al., 2009; Nomura et al., 2004). Such loss leads to the generation of a metaplastic cell lineage derived from chief cells, called SPEM (spasmolytic polypeptide-expressing metaplasia) (Nam et al., 2010). This activation of chief cells is another example of the capacity of mature chief cells to re-enter the cell cycle. The generation of the SPEM cell lineage can also be seen as a reverse transformation of chief cells toward mucous neck cells, as the SPEM lineage expresses markers of both lineages (Capoccia et al., 2013). Chief cells thus react upon damage with proliferation and with changes in their differentiation state. Our lineage-tracing-based observations of stem cell-like behavior of chief cells might thus constitute a physiological equivalent of the SPEM process.

What might explain this unusual phenomenon? The proposed location of the more active, ''workhorse'' stem cell population in the isthmus is unique compared to other stem cell niches in the gastrointestinal tract. The stem cells of the pylorus, small intestine, and colon all reside at the bottoms of epithelial invaginations, farthest away from the potentially harmful contents of the lumen. The isthmus is thus less well protected against damaging agents. A quiescent stem-like cell, such as the *Troy*$^+$ chief cell at the bottom, might serve as back-up to a vulnerable, active stem cell niche located closer to the lumen.

Taken together, *Troy*$^+$ chief cells at gland bottoms can serve as quiescent stem-like cells in the epithelium of the gastric corpus. As has been proposed for other self-renewing tissues (Li and Clevers, 2010), the gastric corpus thus appears to contain two stem cell populations: an actively dividing population located in the isthmus (that remains to be specifically identified) and a small population of ''reserve'' stem-like chief cells, marked by *Troy*, at the gland base. The unique property of the *Troy*$^+$ cell as a fully differentiated cell with the capability to act as a multipotent stem cell represents a surprising example of plasticity in epithelial stem cell biology.

EXPERIMENTAL PROCEDURES

Details on procedures can be found in the Extended Experimental Procedures.

Mice and Treatments

Troy-ki mice were generated by homologous recombination in embryonic stem cells targeting an *eGFP-ires-CreERT2* cassette at the translational start site of *Tnfrsf19* (Figure S1A). Cre-recombinase was activated in *Troy-ki*$^{+/ki}$;*RosaLacZ reporter*$^{+/Rep}$ mice by injecting intraperitoneally 5 mg/20 g mouse weight tamoxifen (Sigma, T5648). For 5-FU treatment, mice were injected with 150 mg/kg of 5-FU (Sigma, F6627) by intraperitoneal injection. *Mist1-CreERT2* mice (Shi et al., 2009) were crossed to the Rosa-mTmG reporter line (Muzumdar et al., 2007). Tamoxifen (1 mg/20 g; Sigma) was injected intraperitoneally every other day for a week (three injections total) to induce GFP induction.

Confocal Analysis of eGFP Expression in Near-Native Tissue Sections

Vibratome sections were prepared from *Troy-ki* and *Lgr5-DTR:eGFP* stomachs and analyzed by confocal microscopy for eGFP expression.

Single-Molecule mRNA In Situ Hybridization

Single-molecule mRNA in situ hybridization was performed as described before (Raj et al., 2008). Probe libraries consisted of typically 48 probes with 20 bp of length complementary to the coding sequence.

Detection of β-Galactosidase Activity and Quantification

Detection of β-galactosidase was performed by X-Gal staining. One hundred gastric units were counted, and the positions of LacZ$^+$ cells from the bottom of glands were noted 1 day, 1 month, and 3 months p.i. Quantification of LacZ$^+$ clone size was performed in 100 gastric units at 1 day, 1 month, 3 months, and 1.5 years p.i. For the number of tracings that reached the lumen, LacZ$^+$ clones in ten adjacent sections were counted.

IHC and Confocal Imaging

Paraffin and cryosections were prepared according to standard protocols. For primary and secondary antibody details, see the Extended Experimental Procedures. *Mist1-CreERT2* tracings were imaged with either Apotome 2 optical sectioning on a Zeiss Axiovert or a custom-built two-photon microscope (Kao et al., 2010).

Immunoelectron Microscopy

GFP expression was detected using cryo-immuno gold staining (Peters et al., 2006).

Gastric Unit Isolation and FACS

Gastric units were isolated by incubation with EDTA, and single cells prepared by trypsinization. *Troy-eGFP*$^+$ large and small cells as well as *Mist1-eGFP*$^+$ cells (after induction of *Mist1-CreERT2;Rosa-mTmG* mice) could be readily differentiated by flow cytometry and gating on FL3 and GFP (Figure 6A) or Tomato-Red and GFP (Figure S5A), respectively.

Gastric Corpus Organoid Culture

Whole gastric glands, FACS-isolated single *Troy-eGFP*$^+$ chief or parietal cells, and *Mist1-eGFP*$^+$ cells were cultured in Matrigel using EGF, Gastrin, FGF10, Noggin, Wnt3a, and R-spondin supplemented culture medium (ENRGFW medium) and passaged weekly. Differentiation toward the pit cell lineage was induced by growing the organoids in Fgf10-, Noggin-, and Wnt-free medium (ERG medium). Tamoxifen was added to the culture medium to induce in vitro lineage tracing. YFP and eGFP were subsequently visualized and recorded in live organoids with confocal microscopy (Leica, SP5).

BrdU and EdU Labeling

BrdU labeling was administered with osmotic pumps. Edu was injected 6, 4, and 2 hr before sacrifice. Paraffin sections were stained with an anti-BrdU antibody, EdU detected by a Click-iT reaction, and sections visualized by confocal microscopy.

Microarray Analysis

Expression profiling was performed on Affymetrix chips with sorted *Troy*$^+$ chief cells (gate A in Figure 6), whole corpus glands, and organoids grown in either ENRGFW or ERG medium and analyzed with the R2 web application (http://r2.amc.nl).

ACCESSION NUMBERS

Array data are available at Gene Expression Omnibus (GEO) under the accession number GSE44060.

SUPPLEMENTAL INFORMATION

Supplemental Information includes Extended Experimental Procedures, six figures, and one table and can be found with this article online at http://dx.doi.org/10.1016/j.cell.2013.09.008.

AUTHOR CONTRIBUTIONS

D.E.S., B.-K.K., and H.C. conceived, designed, and analyzed the experiments. D.E.S. constructed the *Troy-ki* mouse. D.E.S. and B.-K.K. performed the lineage-tracing experiments and analyzed the data. Organoid experiments were conceived, performed, and analyzed by M.H. *Mist1* experiments were conceived, performed, and analyzed by G.S., J.H.G., and J.C.M. Confocal microscopy of cell-cycle dynamics was performed by O.B. Single-molecule mRNA in situ data were generated by A.L. Electron microscopy was performed by P.K. and P.J.P. Analysis of *Lgr5-eGFP:DTR*, *Axin2-LacZ* mice and qPCRs were performed by S.B. Bioinformatic support was provided by J.K. Data interpretation was aided by J.H.v.E. and M.v.d.W. The manuscript was written by D.E.S., B.-K.K., and H.C. and commented on by all other authors.

ACKNOWLEDGMENTS

This work was supported by grants from the Centre for Biomedical Genetics (CBG) to D.E.S.; the European Research Council (EU/232814-StemCellMark), the National Research Foundation of Korea (NRF2011-357-C00093), and the Wellcome Trust (097922/C/11/Z) to B.-K.K.; an EU Marie Curie Fellowship (EU/236954-ICSC-Lgr5) to M.H.; the Cancer Genomics Center (CGCII) to O.B.; an EU Marie Curie Fellowship (EU/300686-InfO) to S.B.; a grant from TI Pharma (T3-106) to J.H.v.E.; the European Research Council (EU/Health-F4-2007-200720) to M.v.d.W.; and DK094989, 2P30 DK052574 to J.C.M. We would like to thank R. Siegmund for graphical abstract design, Mark J. Miller and the Washington University School of Medicine In vivo Imaging Core (IVIC) for help with two-photon imaging, the Washington University Digestive Disease Core Center (DDRCC) Advanced Imaging and Tissue Analysis Core and Shradha Khurana for help in figure preparation, James Goldenring for constructive discussion, and Frederic J. de Sauvage for Lgr5-DTR:eGFP mice.

Received: February 5, 2013
Revised: July 5, 2013
Accepted: September 5, 2013
Published: October 10, 2013

REFERENCES

Arnold, K., Sarkar, A., Yram, M.A., Polo, J.M., Bronson, R., Sengupta, S., Seandel, M., Geijsen, N., and Hochedlinger, K. (2011). Sox2(+) adult stem and progenitor cells are important for tissue regeneration and survival of mice. Cell Stem Cell *9*, 317–329.

Barker, N., van Es, J.H., Kuipers, J., Kujala, P., van den Born, M., Cozijnsen, M., Haegebarth, A., Korving, J., Begthel, H., Peters, P.J., and Clevers, H. (2007). Identification of stem cells in small intestine and colon by marker gene Lgr5. Nature *449*, 1003–1007.

Barker, N., Huch, M., Kujala, P., van de Wetering, M., Snippert, H.J., van Es, J.H., Sato, T., Stange, D.E., Begthel, H., van den Born, M., et al. (2010). Lgr5(+ve) stem cells drive self-renewal in the stomach and build long-lived gastric units in vitro. Cell Stem Cell *6*, 25–36.

Batlle, E., Henderson, J.T., Beghtel, H., van den Born, M.M., Sancho, E., Huls, G., Meeldijk, J., Robertson, J., van de Wetering, M., Pawson, T., and Clevers, H. (2002). Beta-catenin and TCF mediate cell positioning in the intestinal epithelium by controlling the expression of EphB/ephrinB. Cell *111*, 251–263.

Bjerknes, M., and Cheng, H. (2002). Multipotential stem cells in adult mouse gastric epithelium. Am. J. Physiol. Gastrointest. Liver Physiol. *283*, G767–G777.

Bredemeyer, A.J., Geahlen, J.H., Weis, V.G., Huh, W.J., Zinselmeyer, B.H., Srivatsan, S., Miller, M.J., Shaw, A.S., and Mills, J.C. (2009). The gastric epithelial progenitor cell niche and differentiation of the zymogenic (chief) cell lineage. Dev. Biol. *325*, 211–224.

Capoccia, B.J., Jin, R.U., Kong, Y.Y., Peek, R.M., Jr., Fassan, M., Rugge, M., and Mills, J.C. (2013). The ubiquitin ligase Mindbomb 1 coordinates gastrointestinal secretory cell maturation. J. Clin. Invest. *123*, 1475–1491.

Chen, K.Y., and Withers, H.R. (1975). Proliferative capability of parietal and zymogen cells. J. Anat. *120*, 421–432.

Fafilek, B., Krausova, M., Vojtechova, M., Pospichalova, V., Tumova, L., Sloncova, E., Huranova, M., Stancikova, J., Hlavata, A., Svec, J., et al. (2013). Troy, a tumor necrosis factor receptor family member, interacts with Lgr5 to inhibit Wnt signaling in intestinal stem cells. Gastroenterology *144*, 381–391. Published online November 7, 2012. http://dx.doi.org/10.1053/j.gastro.2012.10.048.

Fausto, N. (2000). Liver regeneration. J. Hepatol. *32*(1, Suppl), 19–31.

Goldenring, J.R., Nam, K.T., and Mills, J.C. (2011). The origin of pre-neoplastic metaplasia in the stomach: chief cells emerge from the Mist. Exp. Cell Res. *317*, 2759–2764.

Hashimoto, T., Schlessinger, D., and Cui, C.Y. (2008). Troy binding to lymphotoxin-alpha activates NF kappa B mediated transcription. Cell Cycle *7*, 106–111.

Huh, W.J., Esen, E., Geahlen, J.H., Bredemeyer, A.J., Lee, A.H., Shi, G., Konieczny, S.F., Glimcher, L.H., and Mills, J.C. (2010). XBP1 controls maturation of gastric zymogenic cells by induction of MIST1 and expansion of the rough endoplasmic reticulum. Gastroenterology *139*, 2038–2049.

Huh, W.J., Khurana, S.S., Geahlen, J.H., Kohli, K., Waller, R.A., and Mills, J.C. (2012). Tamoxifen induces rapid, reversible atrophy, and metaplasia in mouse stomach. Gastroenterology *142*, 21–24, e7.

Itzkovitz, S., Lyubimova, A., Blat, I.C., Maynard, M., van Es, J., Lees, J., Jacks, T., Clevers, H., and van Oudenaarden, A. (2012). Single-molecule transcript counting of stem-cell markers in the mouse intestine. Nat. Cell Biol. *14*, 106–114.

Jaks, V., Barker, N., Kasper, M., van Es, J.H., Snippert, H.J., Clevers, H., and Toftgård, R. (2008). Lgr5 marks cycling, yet long-lived, hair follicle stem cells. Nat. Genet. *40*, 1291–1299.

Kao, J.Y., Zhang, M., Miller, M.J., Mills, J.C., Wang, B., Liu, M., Eaton, K.A., Zou, W., Berndt, B.E., Cole, T.S., et al. (2010). Helicobacter pylori immune escape is mediated by dendritic cell-induced Treg skewing and Th17 suppression in mice. Gastroenterology *138*, 1046–1054.

Karam, S.M. (1993). Dynamics of epithelial cells in the corpus of the mouse stomach. IV. Bidirectional migration of parietal cells ending in their gradual degeneration and loss. Anat. Rec. *236*, 314–332.

Karam, S.M., and Leblond, C.P. (1993a). Dynamics of epithelial cells in the corpus of the mouse stomach. I. Identification of proliferative cell types and pinpointing of the stem cell. Anat. Rec. *236*, 259–279.

Karam, S.M., and Leblond, C.P. (1993b). Dynamics of epithelial cells in the corpus of the mouse stomach. III. Inward migration of neck cells followed by progressive transformation into zymogenic cells. Anat. Rec. *236*, 297–313.

Koo, B.K., Spit, M., Jordens, I., Low, T.Y., Stange, D.E., van de Wetering, M., van Es, J.H., Mohammed, S., Heck, A.J., Maurice, M.M., and Clevers, H. (2012). Tumour suppressor RNF43 is a stem-cell E3 ligase that induces endocytosis of Wnt receptors. Nature *488*, 665–669.

Lerner, C., and Harrison, D.E. (1990). 5-Fluorouracil spares hemopoietic stem cells responsible for long-term repopulation. Exp. Hematol. *18*, 114–118.

Li, L., and Clevers, H. (2010). Coexistence of quiescent and active adult stem cells in mammals. Science *327*, 542–545.

Lustig, B., Jerchow, B., Sachs, M., Weiler, S., Pietsch, T., Karsten, U., van de Wetering, M., Clevers, H., Schlag, P.M., Birchmeier, W., and Behrens, J. (2002). Negative feedback loop of Wnt signaling through upregulation of conductin/axin2 in colorectal and liver tumors. Mol. Cell. Biol. *22*, 1184–1193.

Masaki, T., Qu, J., Cholewa-Waclaw, J., Burr, K., Raaum, R., and Rambukkana, A. (2013). Reprogramming adult Schwann cells to stem cell-like cells by leprosy bacilli promotes dissemination of infection. Cell *152*, 51–67.

Michalopoulos, G.K., and DeFrances, M.C. (1997). Liver regeneration. Science *276*, 60–66.

Mills, J.C., and Shivdasani, R.A. (2011). Gastric epithelial stem cells. Gastroenterology *140*, 412–424.

Muñoz, J., Stange, D.E., Schepers, A.G., van de Wetering, M., Koo, B.K., Itzkovitz, S., Volckmann, R., Kung, K.S., Koster, J., Radulescu, S., et al. (2012). The Lgr5 intestinal stem cell signature: robust expression of proposed quiescent '+4' cell markers. EMBO J. *31*, 3079–3091.

Muzumdar, M.D., Tasic, B., Miyamichi, K., Li, L., and Luo, L. (2007). A global double-fluorescent Cre reporter mouse. Genesis *45*, 593–605.

Nam, K.T., Lee, H.J., Sousa, J.F., Weis, V.G., O'Neal, R.L., Finke, P.E., Romero-Gallo, J., Shi, G., Mills, J.C., Peek, R.M., Jr., et al. (2010). Mature chief cells are cryptic progenitors for metaplasia in the stomach. Gastroenterology *139*, 2028–2037, e9.

Nomura, S., Baxter, T., Yamaguchi, H., Leys, C., Vartapetian, A.B., Fox, J.G., Lee, J.R., Wang, T.C., and Goldenring, J.R. (2004). Spasmolytic polypeptide expressing metaplasia to preneoplasia in H. felis-infected mice. Gastroenterology *127*, 582–594.

Peters, P.J., Bos, E., and Griekspoor, A. (2006). Cryo-immunogold electron microscopy. Curr. Prot.Cell Biol. *Chapter 4*, Unit 4.7.

Qiao, X.T., and Gumucio, D.L. (2011). Current molecular markers for gastric progenitor cells and gastric cancer stem cells. J. Gastroenterol. *46*, 855–865.

Qiao, X.T., Ziel, J.W., McKimpson, W., Madison, B.B., Todisco, A., Merchant, J.L., Samuelson, L.C., and Gumucio, D.L. (2007). Prospective identification of a multilineage progenitor in murine stomach epithelium. Gastroenterology *133*, 1989–1998.

Quante, M., Marrache, F., Goldenring, J.R., and Wang, T.C. (2010). TFF2 mRNA transcript expression marks a gland progenitor cell of the gastric oxyntic mucosa. Gastroenterology *139*, 2018–2027, e2.

Raj, A., van den Bogaard, P., Rifkin, S.A., van Oudenaarden, A., and Tyagi, S. (2008). Imaging individual mRNA molecules using multiple singly labeled probes. Nat. Methods *5*, 877–879.

Ramsey, V.G., Doherty, J.M., Chen, C.C., Stappenbeck, T.S., Konieczny, S.F., and Mills, J.C. (2007). The maturation of mucus-secreting gastric epithelial progenitors into digestive-enzyme secreting zymogenic cells requires Mist1. Development *134*, 211–222.

Shao, Z., Browning, J.L., Lee, X., Scott, M.L., Shulga-Morskaya, S., Allaire, N., Thill, G., Levesque, M., Sah, D., McCoy, J.M., et al. (2005). TAJ/TROY, an orphan TNF receptor family member, binds Nogo-66 receptor 1 and regulates axonal regeneration. Neuron *45*, 353–359.

Shi, G., Zhu, L., Sun, Y., Bettencourt, R., Damsz, B., Hruban, R.H., and Konieczny, S.F. (2009). Loss of the acinar-restricted transcription factor Mist1 accelerates Kras-induced pancreatic intraepithelial neoplasia. Gastroenterology *136*, 1368–1378.

Tashima, K., Zhang, S., Ragasa, R., Nakamura, E., Seo, J.H., Muvaffak, A., and Hagen, S.J. (2009). Hepatocyte growth factor regulates the development of highly pure cultured chief cells from rat stomach by stimulating chief cell proliferation in vitro. Am. J. Physiol. Gastrointest. Liver Physiol. *296*, G319–G329.

Tian, H., Biehs, B., Warming, S., Leong, K.G., Rangell, L., Klein, O.D., and de Sauvage, F.J. (2011). A reserve stem cell population in small intestine renders Lgr5-positive cells dispensable. Nature *478*, 255–259.

Van der Flier, L.G., Sabates-Bellver, J., Oving, I., Haegebarth, A., De Palo, M., Anti, M., Van Gijn, M.E., Suijkerbuijk, S., Van de Wetering, M., Marra, G., and Clevers, H. (2007). The intestinal Wnt/TCF signature. Gastroenterology *132*, 628–632.

van der Flier, L.G., van Gijn, M.E., Hatzis, P., Kujala, P., Haegebarth, A., Stange, D.E., Begthel, H., van den Born, M., Guryev, V., Oving, I., et al. (2009). Transcription factor achaete scute-like 2 controls intestinal stem cell fate. Cell *136*, 903–912.

Willems, G., Galand, P., Vansteenkiste, Y., and Zeitoun, P. (1972). Cell population kinetics of zymogen and parietal cells in the stomach of mice. Z. Zellforsch. Mikrosk. Anat. *134*, 505–518.

Wong, V.W., Stange, D.E., Page, M.E., Buczacki, S., Wabik, A., Itami, S., van de Wetering, M., Poulsom, R., Wright, N.A., Trotter, M.W., et al. (2012). Lrig1 controls intestinal stem-cell homeostasis by negative regulation of ErbB signalling. Nat. Cell Biol. *14*, 401–408.